

Geophysical Research Letters

RESEARCH LETTER

10.1029/2018GL081370

Key Points:

- The spring phenology will become more spatially synchronous across the Northern Hemisphere
- Larger advances in spring phenology at high latitudes than the low latitudes are estimated under future climatic warming scenarios
- The increased synchrony is due to both fast spring warming and slow decline in temperature sensitivity of spring phenology at high latitudes

Supporting Information:

- Supporting Information S1
- Table S1

Correspondence to:

S. Piao,
slpiao@pku.edu.cn

Citation:

Liu, Q., Piao, S., Fu, Y. H., Gao, M., Peñuelas, J., & Janssens, I. A. (2019). Climatic warming increases spatial synchrony in spring vegetation phenology across the Northern Hemisphere. *Geophysical Research Letters*, 46, 1641–1650. <https://doi.org/10.1029/2018GL081370>







Received 23 NOV 2018

Accepted 11 JAN 2019

Accepted article online 18 JAN 2019

Published online 5 FEB 2019

Climatic Warming Increases Spatial Synchrony in Spring Vegetation Phenology Across the Northern Hemisphere

Qiang Liu¹ , Shilong Piao^{1,2,3} , Yongshuo H. Fu^{1,4} , Mengdi Gao¹ , Josep Peñuelas^{5,6} , and Ivan A. Janssens⁴ 

¹Sino-French Institute for Earth System Science, College of Urban and Environmental Sciences, Peking University, Beijing, China, ²Key Laboratory of Alpine Ecology and Biodiversity, Institute of Tibetan Plateau Research, Chinese Academy of Sciences, Beijing, China, ³Center for Excellence in Tibetan Earth Science, Chinese Academy of Sciences, Beijing, China, ⁴Department of Biology, University of Antwerp, Wilrijk, Belgium, ⁵CREAF, Cerdanyola del Valles, Barcelona, Spain, ⁶CSIC, Global Ecology Unit CREAM-CSIC-UAB, Barcelona, Spain

Abstract Climatic warming has advanced spring phenology across the Northern Hemisphere, but the spatial variability in temperature sensitivity of spring phenology is substantial. Whether spring phenology will continue to advance uniformly at latitudes has not yet been investigated. We used Bayesian model averaging and four spring phenology models, and demonstrated that the start of vegetation growing season across the Northern Hemisphere will become substantially more synchronous (up to 11.3%) under future climatic warming conditions. Larger start of growing season advances are expected at higher than lower latitudes (3.7–10.9 days earlier) due to both larger rate in spring warming at higher latitudes and larger decreases in the temperature sensitivity of start of growing season at low latitudes. The consequent impacts on the northern ecosystems due to this increased synchrony may be considerable and thus worth investigating.

Plain Language Summary Recent climatic warming has not only triggered a notable advance of spring phenology over the past decades but also changed the spatial pattern of its temperature sensitivity. Whether the shifts in spring phenology would continue to follow the latitude gradient remains unclear. Based on simulations over the end of this century, we concluded that the advance of spring phenology at high latitudes is larger than the low latitudes, consequently resulting in more synchronous spring phenology. Further analysis suggests that besides greater spring warming at high latitudes, the larger decrease in temperature sensitivity of spring phenology possibly due to shorter day length and chilling loss at low latitudes also contributes to this finding. Our study, therefore, reports the possibility of improving phenological modules in dynamic vegetation models and thus promoting our understanding of the response of northern ecosystem to ongoing climate change.

1. Introduction

The rising spring temperatures in recent decades have led to a notable advance of spring phenology over the Northern Hemisphere (NH; Fu et al., 2016; Menzel et al., 2006; Peñuelas & Filella, 2001; Piao et al., 2015; Schwartz et al., 2006), which has substantially affected terrestrial water, carbon, and nutrient balances (Keenan et al., 2014; Peñuelas & Filella, 2009; Piao et al., 2007, 2017; Richardson et al., 2010). A recent study reported a declining response of spring phenology to warming temperature, attributed to winter chilling loss (Fu et al., 2015) and questioning whether spring phenology across different regions would continue to advance as climate warms. Extrapolating current knowledge on the bioclimatic gradient in spring phenology (e.g., a progressive delay in spring phenology with increasing latitude, “Hopkin’s bioclimatic law”; Hopkins, 1920, 1938) to the future is therefore challenging. Recent studies have reported an increase in synchrony of spring phenology (i.e., reduced differences between the start of growing season (SOS) among species) in recent decades from in situ observations at regional scales (C. Wang et al., 2016) and along altitudinal gradients (Vitasse et al., 2018), attributed to spatial differences in warming speed and phenological responses to rising temperature. Whether such increasing synchrony continues to occur across the entire NH under warmer scenarios, however, has not yet been investigated. We quantified the changes in the spatial variance of spring phenology across the NH under current and future conditions based on model simulations to explore the changes in the synchrony of SOS.

Models of spring phenology have been widely used to reproduce SOS in previous studies (Jeong et al., 2013; Liu et al., 2018; Melaas et al., 2015), but considerable uncertainties nonetheless remain within and among models due to limited understanding of mechanisms underlying spring phenology (Chuine & Régnière, 2017; Richardson et al., 2012). Multiple model predictions, combining the strengths of individual models and reducing the computed uncertainties, are therefore required, although comprehensive understanding of spring phenology still need well-designed experimental studies. Previous multimodel studies simply assigned equal weights to all models, regardless of their performance, and calculated their ensemble mean (i.e., simple model averaging (SMA)). We, however, applied Bayesian model averaging (BMA) to deal with individual model uncertainty by assigning higher weights to models with higher accuracies in the observational period. Four models of spring phenology (see section 2), were applied to simulate SOS over the NH under current (1990–2009) and future (2080–2099; four Representative Concentration Pathways (RCPs)) conditions.

2. Materials and Methods

2.1. Climatic Data Sets

Daily mean temperature (T) was obtained from the CRU-NCEP (Climatic Research Unit (CRU) and National Centers for Environmental Protection (NCEP)) v5 data set at a spatial resolution of $0.5 \times 0.5^\circ$ for 1982–2012. This data set combines the CRU-TS (time series) v3.1 $0.5 \times 0.5^\circ$ monthly climatological data (1901–2012) and the NCEP reanalysis at $2.5 \times 2.5^\circ$ and a 6-hr time interval since 1948 (Mitchell & Jones, 2005; New et al., 2000). For future projections, we acquired data for daily T from predictions by Coupled Model Intercomparison Project phase 5 models (Table S1). The Coupled Model Intercomparison Project phase 5 model predictions for the historical (1980–2005), RCP2.6, RCP4.5, RCP6.0, and RCP8.5 (2006–2009 and 2070–2099) scenarios were processed and interpolated to a spatial resolution of $1 \times 1^\circ$ using Climate Data Operators (Schulzweida, 2013).

2.2. Satellite-Derived SOS

In this study, we extracted SOS from the latest Normalized Difference Vegetation Index (NDVI) data set by NASA's GIMMS group (NDVI_{3g,v1}) at a spatial resolution of $1/12 \times 1/12^\circ$ spanning the period 1982–2012. Apart from the issues which have already been addressed in NDVI_{3g} (e.g., update of satellite sensors, atmospheric interference, and nonvegetation dynamics; Pinzon & Tucker, 2014), artifacts due to snow coverage and changes in calibration were further processed in NDVI_{3g,v1}. The SOS extraction methods include two main steps: (1) reconstructing NDVI time series to a daily basis using data filter function and (2) determining SOS from predefined thresholds or changing characteristics of the filtered NDVI curve. Following Liu, Fu, Zeng, et al. (2016) and Liu, Fu, Zhu, et al. (2016), we estimated the date of SOS using four commonly used methods (i.e., Hants-Mr (Jakubauskas et al., 2001), Polyfit-Mr (Piao et al., 2006), double logistic (Julien & Sobrino, 2009), and piecewise logistic (Zhang et al., 2003)). To reduce the uncertainty resulted from inter-method differences, we applied SOS averaged from four methods in our analysis.

2.3. Models of Spring Phenology

We used four models of spring phenology involving both endodormancy and ecodormancy phases. These models assume that chilling and forcing (subsequent to chilling) are required to break endodormancy and ecodormancy, respectively, and define the day when the accumulation of forcing becomes critical as the date of leaf unfolding (Cannell & Smith, 1983; Murray et al., 1989). The four models include three temperature-driven models, that is, the Sequential Model (Hänninen, 1990; Kramer, 1994), Unified Model, and UniChill Model (I. Chuine, 2000). Besides, the DORMPHOT model additionally considered the effect of photoperiod and assumed that reduced temperature and photoperiod co-triggered dormancy, and a long day length would promote the accumulation of forcing (Caffarra, Donnelly, & Chuine, 2011). These models were calibrated using satellite-derived SOS and daily temperature at plant function type (MacBean et al., 2015) scale for the period 1982–2012 using Bayesian optimization technique (Martinez-Cantin, 2014). The detailed model implementation could be found in Table S2 and Text S1.

2.4. BMA

Previous studies have mostly been based on results from either a single model of spring phenology or the average of multiple models. Simple model averaging (SMA) is superior to a single model but does not

identify the best model. BMA, however, assigns higher weights to models that have previously performed better and is therefore able to obtain the minimum root-mean-square error between the weighted model ensemble and observations (Raftery & Zheng, 2003). We applied BMA to determine the optimal weight for each model of spring phenology at a pixel level for 1982–2012. Supposing that SOS anomaly was forecasted by on the basis of training data SOS^T anomaly (randomly selected as 80% from the entire study period), using models of spring phenology (M_1, \dots, M_k), then the forecast probability density function, $p(SOS)$, is written as

$$p(SOS) = \sum_{k=1}^K p(SOS|M_k)p(M_k|SOS^T) \quad (1)$$

where $p(SOS|M_k)$ is the normal conditional probability density function based on model M_k and $p(M_k|SOS^T)$ is the posterior probability of model M_k , which is corrected by the training data and also indicates how well model M_k fits the training data (i.e., weight of each model). This term can be calculated as

$$p(M_k|SOS^T) = \frac{p(SOS^T|M_k)p(M_k)}{\sum_{l=1}^k p(SOS^T|M_l)p(M_l)} \quad (2)$$

where $p(M_k)$ is the prior probability of model M_k . We defined the probability of the training data (e.g., SOS^T anomaly) as the likelihood function following Raftery et al. (2005), the optimal weights (e.g., $p(M_k|SOS^T)$) were determined when the likelihood function reached its maximum. More details about BMA are provided by Raftery et al. (2005) and Vrugt and Robinson (2007).

2.5. Sensitivity of Spring Phenology to Temperature

We calculated the sensitivity (S_T) of SOS to mean spring temperature (T_{spr}) as the ratio between changes in SOS (ΔSOS) and changes in T_{spr} (ΔT_{spr}) during 2080–2099 and 1990–2009:

$$S_T = \Delta SOS / \Delta T_{spr} \quad (3)$$

We calculated BMA-based SOS for each year over these two periods. T_{spr} for individual years was calculated as the average of daily mean temperature from 1 March to 31 May. We assessed the influence of future warming on SOS by calculating S_T across the NH under four RCPs. We first calculated ΔSOS and ΔT_{spr} for each model and then applied their ensemble mean to reduce the uncertainties within predictions by the Coupled Model Intercomparison Project phase 5 models (Table S1).

2.6. Analysis

We ran the models of spring phenology under five independent scenarios to investigate whether the response of SOS to temperature might be constrained by shorter photoperiod as SOS continues to advance or chilling loss due to winter warming. We chose the DORMPHOT model to test the effect of photoperiod. We first ran this model with the actual photoperiod (S1), then increased the photoperiod during spring (March–May) by 1 and 3 hr, individually (S2). The remaining simulations were carried over all four models. We calculated winter temperature from 1 September of the previous year to 31 January of the current year, because the accumulation of chilling begins on 1 September of the previous year in these models. In the third scenario (S3), we randomly selected winter temperature from 1982 to 2009 and kept it constant during 2080–2099. Similarly, we considered varying winter temperature but kept spring temperature (March–May) constant during 2080–2099 (S4). To reduce the sampling bias, we additionally ran S3 and S4 for 9 times and applied the average of 10 simulations in our analysis. In the fifth scenario (S5), we considered varying winter and spring temperature for 2080–2099. We thereafter calculated BMA-based SOS projections for 2080–2099 and then the differences among these scenarios. We conducted this analysis based on temperature projections from four RCPs to test the influence of longer photoperiod (S2-S1), winter warming (S3-S5), and spring warming (S4-S5) on the date of SOS.

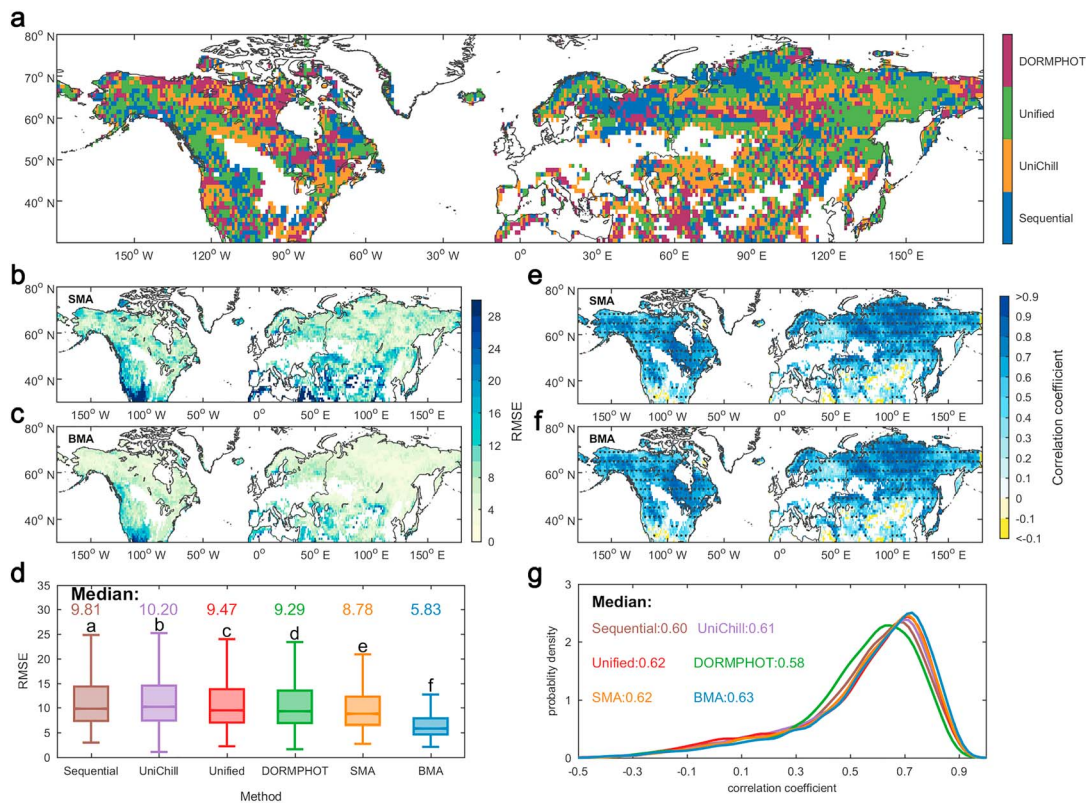


Figure 1. Bayesian model averaging (BMA) of simulated start of the growing season (SOS) for 1982–2012 and its comparison with simple model averaging (SMA) and four models. (a) The optimal selection among models based on weight inferred from BMA. (b and c) Root-mean-square error (RMSE) and (e and f) temporal correlations between simulated and satellite-derived SOS. (d) The box plots of RMSEs for the individual models, SMA and BMA. (g) The probability distribution of correlation coefficients across the NH. Different letters in (d) indicate significant differences at $p < 0.05$ using nonparametric Kruskal-Wallis tests followed by Bonferroni post hoc tests.

3. Results and Discussion

3.1. BMA

The weight assigned by BMA served as a good criterion for model evaluation for 1982–2012. The Unified Model performed best in ~30% of the NH, that is, northeastern Siberia and western North America. The UniChill and Sequential Models produced the best agreement with satellite-derived SOS in ~25 and 24% of the NH, respectively. The UniChill Model outperformed the other models in central Eurasia, and the Sequential Model performed the best in northeastern Europe and northern Siberia. The DORMPHOT model agreed best in ~21% of the NH, albeit fragmentally distributed (Figure 1a). Plants differ across the regions, and species differ in their response to chilling, photoperiod, and spring warming, so different models are likely to be better for different regions. Benefiting from the strength of individual models, the BMA-based SOS simulations were in better agreement with satellite observations across the NH. As expected, root-mean-square errors were consistently lower compared to simulations based on either SMA or the single models, particularly over southwestern North America and central Eurasia (Figures 1b–1d and S1). The median root-mean-square error decreased substantially from 9.3–10.2 days for the individual models to 8.8 days for SMA and 5.8 days for BMA (Figure 1d). These differences were less apparent in the temporal correlations between the simulated and satellite-derived SOSs (Figures 1e–1g and S2).

3.2. Projected Changes in Spring Phenology and Its Synchrony

SOS across the NH was obtained for 2080–2099 by extrapolating the same weights of the phenological models to future simulations. Regionally different responses to the projected climate change were obtained (Figures 2 and S4; based on ensemble mean of model projections under each RCP, because the intermodel differences showed similar magnitude) (Figure S3). SOS was generally significantly earlier in most of the NH

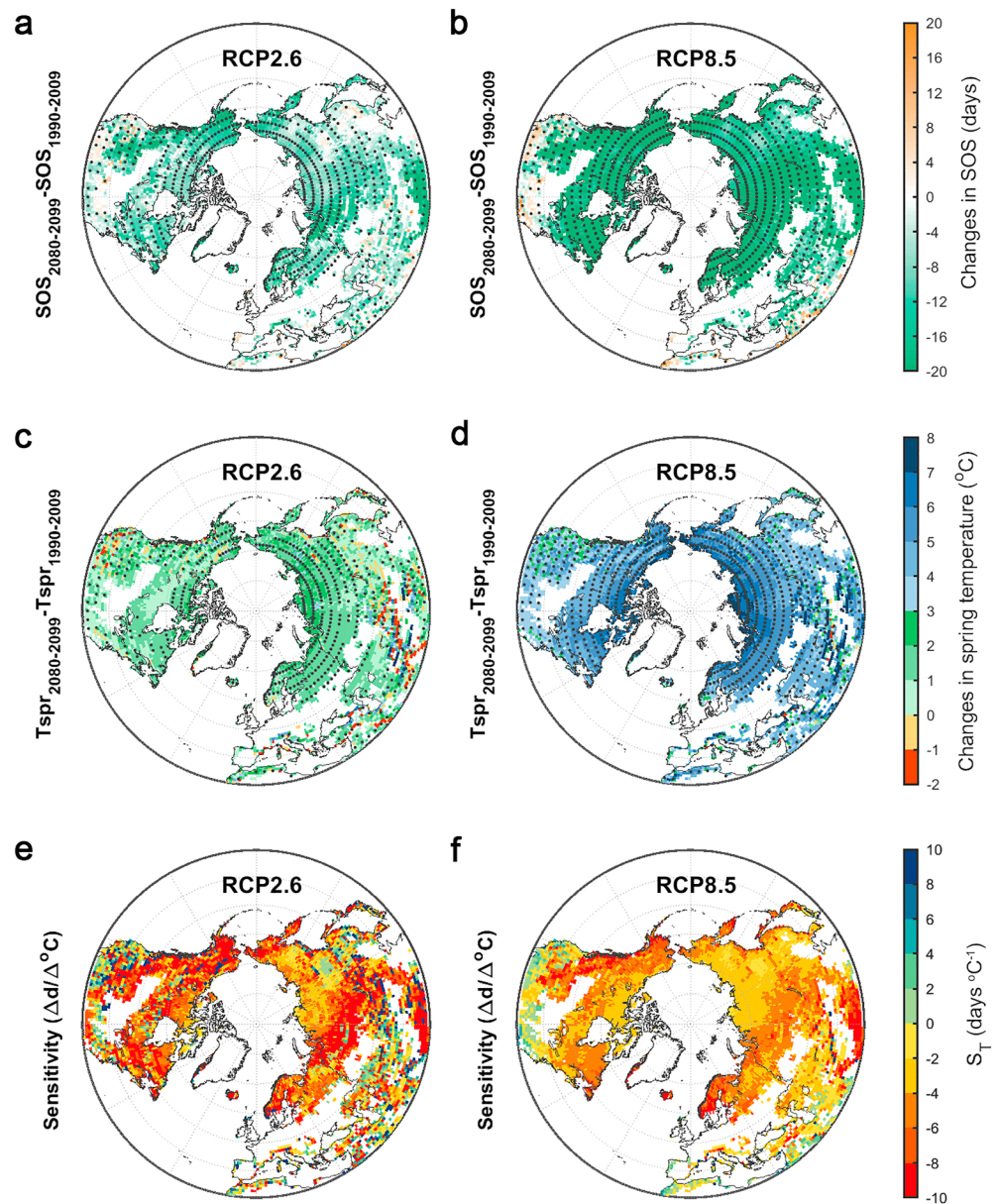


Figure 2. Changes of SOS and spring temperature between 1980–2009 and 2080–2099. The top panels show the changes of BMA-based SOS predictions under two representative concentration pathways (RCPs), (a) RCP2.6 and (b) RCP8.5. The middle panels show changes in mean spring temperature (T_{spr}) under (c) RCP2.6 and (d) RCP8.5. Regions marked with black dots indicate statistically significant ($p < 0.05$, t test) changes in SOS (a and b) and spring temperature (c and d). Figures (e) and (f) indicate the temperature sensitivity (S_T) of SOS to spring warming under two RCPs.

(ranging from 75% in RCP2.6 to 91% in RCP8.5, $p < 0.05$) between 2080–2099 and 1990–2009. SOS, however, was sometimes also delayed, especially under warmer scenarios in the low latitudes (e.g., 30–50°N; Figures 2a, 2b, 3a, and 3b). SOS across the NH was 7.9 ± 6.8 days (RCP2.6) to 19.1 ± 12.3 days (RCP8.5) earlier (average \pm SD) during 2080–2099 than the current period (1990–2009). SOS under RCP2.6 scenario advanced more (e.g., >12 days) at high latitudes (e.g., northwestern North America, northern Europe, northern Siberia) and the Tibetan Plateau, followed by low latitudes (e.g., southeastern Siberia and central Eurasia; Figure 2a). This spatial pattern of faster SOS advances at higher than lower latitudes was more apparent under warmer RCPs. For example, the difference in the average SOS advancement between higher and low latitudes increased from 4 days under RCP2.6 to 11 days under RCP8.5 (Figures 2b, S4a, S4b, 3a, 3b, S5a, and S5b).

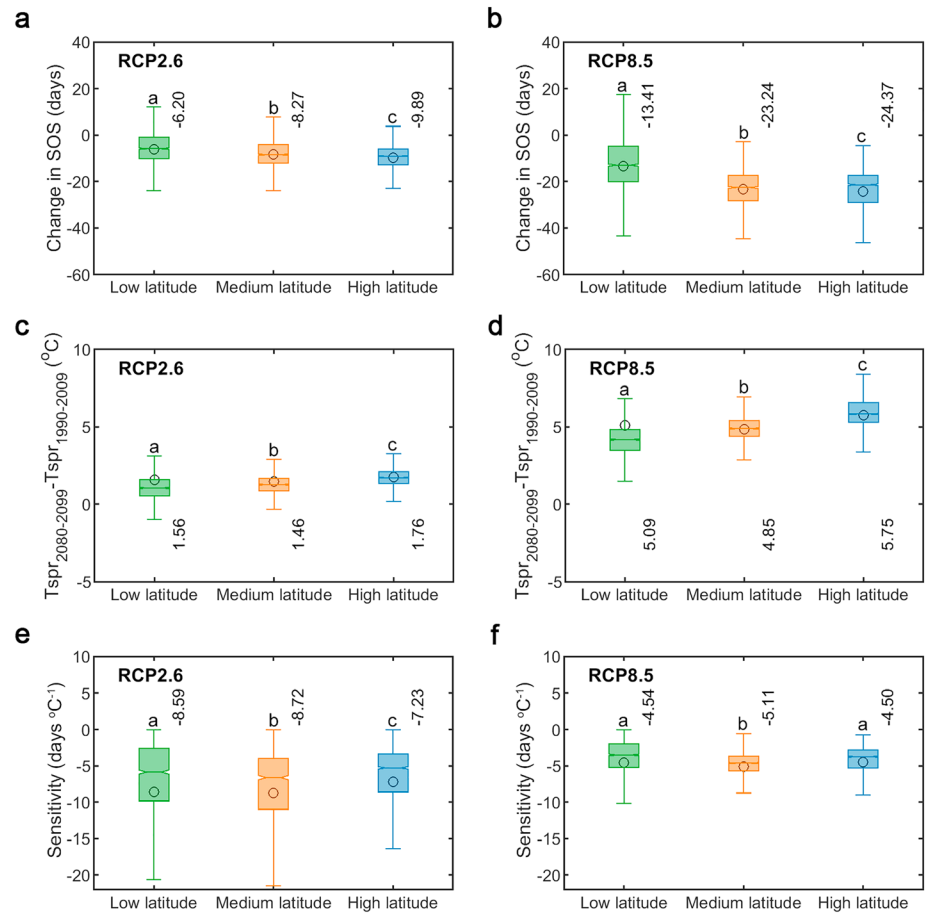


Figure 3. Changes in BMA-based SOS and spring warming for 2080–2099 compared to 1980–2009 for various latitudinal bands. Box plots indicate the distribution of changes in SOS, changes in T_{spr} , and temperature sensitivity (S_T) at low (30–50°N), medium (50–60°N), and high latitudes (>60°N) under RCP2.6 and RCP8.5, with black circles denoting their averages. Different letters indicate significant differences at $p < 0.05$ using nonparametric Kruskal-Wallis tests followed by Bonferroni post hoc tests.

The weakening latitudinal gradient of SOS under future climatic warming indicated the increasing synchrony of spring phenology across the NH. The spatial standard deviation of SOS decreased by 4.0% from 32.7 days (~99% of 33.0 days based on satellite observations) for 1990–2009 to 31.4 days for 2090–2099 (RCP2.6) and continued to decrease under warmer RCPs, that is, 30.8 days (5.8%, RCP4.5), 30.4 days (7.0%, RCP6.0), and 29.0 days (11.3%, RCP8.5; Figure 4c). We found that the decrease in the spatial variation of SOS was related to the regional differences in the response of vegetation to the future climatic warming. Average SOS for 1990–2009 was significantly negatively correlated ($p < 0.05$) with its projected future change (Figures 4a, 4b, S6a, and S6b), implying that regions with later SOSs at current condition (usually at high latitudes) would likely have larger SOS advances under future climatic warming. These findings were also confirmed by each of the four spring phenology models (Figure S7) and thus indicate that the vegetation across the NH will initiate spring growth more synchronously in the future, especially between the low and high latitudes.

3.3. Determinations of the Increasing Synchrony of Spring Phenology

The increasing synchrony of spring phenology between 2080–2099 and 1990–2009 is co-determined by spring temperature (T_{spr}) and the sensitivity of SOS to spring warming (S_T), which both differ between lower and higher latitudes. S_T was higher at low latitudes (e.g., 30–50°N) than at high latitudes (e.g., >60°N, $p < 0.05$ under most RCPs, Kruskal-Wallis tests followed by Bonferroni post hoc tests; Figures 3e, 3f, S5e, and S5f), in line with results from previous observational studies (Menzel et al., 2006; Wolkovich et al.,

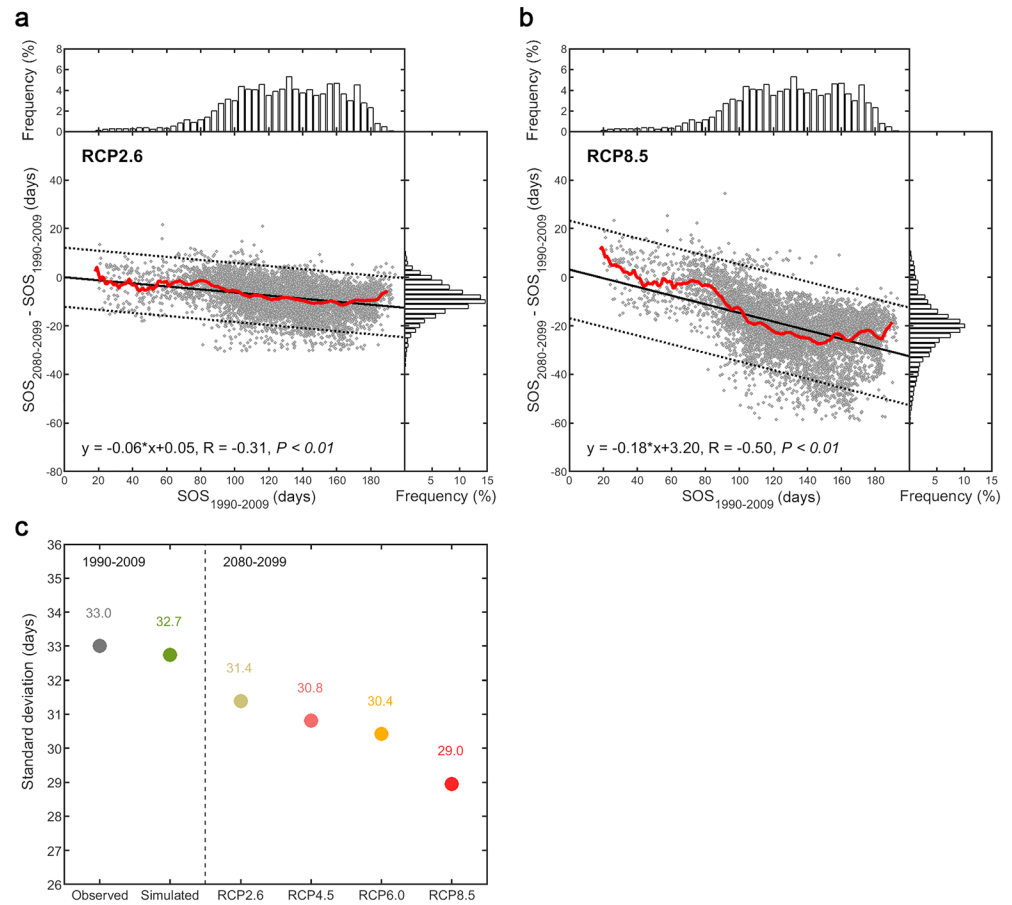


Figure 4. Scatterplots showing the relationship between the average SOS for 1990–2009 and its future change for 2080–2099. (a) Scatterplot based on SOS predictions under RCP2.6. The black line and the two dashed lines indicate the linear regression and its 95% confidence intervals. The red line shows the average changes in SOS within a one-week moving window. The upper and right insets are the frequency distribution of SOS for 1990–2009 and its change from 1990–2009 to 2080–2099. (b) The similar result based on RCP8.5. (c) The standard deviation of SOS across the Northern Hemisphere under current and future conditions.

2012), implying that vegetation at lower latitudes (or with earlier SOS) is more sensitive to changes in T_{spr} . The changes in SOS between these periods nonetheless did not always match the spatial pattern of S_T , because of the much larger increase in T_{spr} at higher latitudes (e.g., 0.2–0.7 °C higher than at low latitudes; Figures 3c, 3d, S5c, and S5d). For example, S_T was lower for northern Siberia than the Tibetan Plateau, but the advance in SOS was similar between these regions due to the faster increase in T_{spr} across northern Siberia (e.g., RCP2.6; Figures 2a and 2e). This finding was consistently confirmed under the remaining RCPs (Figures 2 and S4). Although the S_T was lower at higher latitudes, the faster increasing in T_{spr} could also lead to larger advancement in SOS, thereby reducing the spatial differences in predicted SOS across the NH (e.g., RCP2.6; Figure 2). Moreover, S_T decreased more at lower than higher latitudes across different RCPs. The decrease in S_T between the results under RCP2.6 and RCP8.5 was largest at lower latitudes (30–50°N), averaging 4.1 days/°C (Figures 3e and 3f). The average decrease in S_T at higher latitudes (>60°N), however, was only 2.7 days/°C (Figures 3e and 3f). The comparison between S_T estimated from RCP2.6 and the two intermediate RCPs confirmed this finding (Figures 3e, S5e, and S5f). Greater synchrony in spring phenology is thus projected across the NH (Figure 4c), accompanied with the faster spring warming at the high latitudes (Figures 3c, 3d, S5c, and S5d).

Several hypotheses have been proposed to explain the faster decrease in S_T at low latitudes. A first hypothesis correlates the reduced S_T with the variance of local spring temperature (T_{spr}). A recent ground-based study found that plants at locations with larger T_{spr} variances were less sensitive to warming (T. Wang et al., 2014),

because plants under such conditions tend to depend on more stable environmental cues, such as photoperiod (Körner & Basler, 2010) and/or higher chilling requirement (Schwartz & Hanes, 2010), to avoid premature exposure to damaging spring frost. Such reduction in S_T due to higher T_{spr} variances, however, was not directly implemented in the temperature-based models of phenology and could not be tested.

The hypothesized role for a negative impact of a shorter photoperiod on S_T , however, could be tested across the NH using the DORMPHOT model (Table S2), which involves the effect of photoperiod (Caffarra, Donnelly, & Chuine, 2011). We compared SOS projections over 2080–2099 with actual (S1) and increased (S2) photoperiod (see section 2). The difference between S2 and S1 indicated that increasing photoperiod alone would exacerbate the advance of SOS across most of the NH (>98% (Figures S8a–S8d) and >99% (Figures S8e–S8h), across all RCPs), especially at low latitudes (e.g., southern North America, the Tibetan Plateau) and in northern Europe. The effects of increased photoperiod on advancing SOS decreased significantly toward higher latitudes (Figure S8). This finding not only confirmed the photoperiodic control of SOS (Caffarra, Donnelly, Chuine, & Jones, 2011; Körner & Basler, 2010; Zohner et al., 2016) but also suggested that the shorter days due to earlier SOS might restrict the advance of SOS in the future, particularly at lower latitudes, thus shaping the spatial pattern of a faster decrease in S_T at low latitudes. Photoperiod does not exclusively account for our finding; the other models considering chilling and forcing effects also produced a similar spatial pattern of faster decrease in S_T at lower latitudes (Figure S9).

The control of SOS by cold temperatures during dormancy is a third hypothesis that could account for the regional difference in the future decrease in S_T . We tested this hypothesis by applying four chilling-based models for 2080–2099 but kept the winter temperature (S3) or the spring temperature (S4) constant and then assessing their difference to simulations based on varying winter and spring temperatures (S5; Figures S10a–S10h; see section 2). The warming winter led to a delayed SOS, albeit primarily at lower latitudes (except for the Tibetan Plateau; Figures S10a–S10d). The predicted SOSs across most of the NH (mainly at higher latitudes) did not differ significantly between these two simulations ($p > 0.05$). These findings imply that increasing winter temperatures may indeed lead to insufficient chilling at lower latitudes (except for the Tibetan Plateau), which would subsequently minimize the response of SOS to warming temperatures because of the increasing requirement for forcing temperatures with decreased chilling (Fu et al., 2015; Laube et al., 2014). In contrast, vegetation at high latitudes would still experience sufficient chilling due to the colder and longer winter, and the increasing temperature might even increase its exposure to chilling in regions where temperature was typically below the base temperature for chilling accumulation (Vandvik et al., 2018). Experimental studies comparing phenology in regions at lower and higher elevations have reported similar findings (Gusewell et al., 2017; Vitasse et al., 2018). Large-scale manipulative field or virtual numerical experiments are still required to further test these hypotheses, because the scenarios designed to explain the faster decrease in S_T were less realistic. It should also be noted that our analysis assumes that model bias in the historical period is representative of model performance in the future, and model weights determined under current conditions are preserved for the future. This assumption needs to be tested a wide range of plant species and climatic conditions, because the underlying mechanisms for spring phenology are still not entirely elucidated. For example, photoperiod might influence the spring phenology of some species more strongly under a warmer climate (Körner & Basler, 2010; Way & Montgomery, 2015). In this study, we applied four empirical models, involving chilling, forcing, and photoperiod effects, to account for changes in SOS and observed an increased synchrony in spring phenology. Nonetheless, more efforts should also be placed on experimental studies focused on revealing mechanisms behind the phenological processes (e.g., temperature, photoperiod, and precipitation controls) and improving the predictability of spring phenology models (e.g., Figures 1e and 1f).

4. Conclusions

We report overall advancing, but heterogeneously distributed, trends in spring phenology across the NH between 1990–2009 and 2080–2099 (under four climatic scenarios). The synchrony of spring phenology is expected to increase (i.e., a decrease in spatial variation) across the NH in the future, because projected advances in SOS for 2080–2099 are larger for regions with later SOSs during 1990–2009 (e.g., higher latitudes). This phenomenon is due mainly to the larger increase in spring temperature at high latitudes, which even compensates for the influence of the generally lower S_T at high versus low latitudes. Besides, S_T under

the warmer climatic scenarios decreased more at low latitudes than at high latitudes, probably due to the shorter day length and/or loss of winter chilling, thus amplifying the phenological synchrony as climatic warming proceeds. Changes in the synchrony of spring phenology may result in synchronous change of land-surface physical conditions (e.g., canopy conductance, albedo, and surface aerodynamic roughness) over large areas (Peñuelas & Filella, 2009; Richardson et al., 2013), and thereby surface water fluxes, energy balance, and atmospheric circulation during spring (Peñuelas & Filella, 2009; Stéfanon et al., 2012). To date, most phenological modules in dynamic global vegetation models relied on growing degree days (Sitch et al., 2003; Thornton et al., 2002) or carbon allocation (Ostle et al., 2009) and yielded poor predictions in spring phenology (Richardson et al., 2012). Therefore, updating the bioclimatic gradient of spring phenology (Hopkins, 1920, 1938) across the latitude due to climate change and improving the representation of phenological synchrony in dynamic global vegetation models could enhance our understanding and predictive capacity of how northern ecosystems will respond to a future warmer climate.

Data Availability

All data sets and materials used in this study are freely available online, as described in Table S3.

Acknowledgments

This study was supported by the National Natural Science Foundation of China (41530528), National Youth Top-notch Talent Support Program in China, and the 111 Project (B14001).

References

- Caffarra, A., Donnelly, A., & Chuine, I. (2011). Modelling the timing of *Betula pubescens* budburst. II. Integrating complex effects of photoperiod into process-based models. *Climate Research*, 46(2), 159–170. <https://doi.org/10.3354/cr00983>
- Caffarra, A., Donnelly, A., Chuine, I., & Jones, M. B. (2011). Modelling the timing of *Betula pubescens* budburst. I. Temperature and photoperiod: A conceptual model. *Climate Research*, 46(2), 147–157. <https://doi.org/10.3354/cr00980>
- Cannell, M., & Smith, R. (1983). Thermal time, chill days and prediction of budburst in *Picea sitchensis*. *Journal of Applied Ecology*, 20(3), 951–963. <https://doi.org/10.2307/2403139>
- Chuine, I. (2000). A unified model for budburst of trees. *Journal of Theoretical Biology*, 207(3), 337–347. <https://doi.org/10.1006/jtbi.2000.2178>
- Chuine, I., & Régnière, J. (2017). Process-based models of phenology for plants and animals. *Annual Review of Ecology, Evolution, and Systematics*, 48(1), 159–182. <https://doi.org/10.1146/annurev-ecolsys-110316-022706>
- Fu, Y. H., Liu, Y., De Boeck, H. J., Menzel, A., Nijs, I., Peaucelle, M., et al. (2016). Three times greater weight of daytime than of night-time temperature on leaf unfolding phenology in temperate trees. *New Phytologist*, 212(3), 590–597. <https://doi.org/10.1111/nph.14073>
- Fu, Y. H., Zhao, H., Piao, S., Peaucelle, M., Peng, S., Zhou, G., et al. (2015). Declining global warming effects on the phenology of spring leaf unfolding. *Nature*, 526(7571), 104–107. <https://doi.org/10.1038/nature15402>
- Gusewell, S., Furrer, R., Gehrig, R., & Pietragalla, B. (2017). Changes in temperature sensitivity of spring phenology with recent climate warming in Switzerland are related to shifts of the pre-season. *Global Change Biology*, 23(12), 5189–5202. <https://doi.org/10.1111/gcb.13781>
- Hänninen, H. (1990). Modelling bud dormancy release in trees from cool and temperate regions. *Acta Forestalia Fennica*, (213), 1–47.
- Hopkins, A. D. (1920). The bioclimatic law. *Journal of the Washington Academy of Sciences*, 10(2), 34–40.
- Hopkins, A. D. (1938). Bioclimatics: A science of life and climate relations. US Department of Agriculture.
- Jakubauskas, M. E., Legates, D. R., & Kastens, J. H. (2001). Harmonic analysis of time-series AVHRR NDVI data. *Photogrammetric Engineering and Remote Sensing*, 67(4), 461–470.
- Jeong, S. J., Medvigy, D., Shevliakova, E., & Malyshev, S. (2013). Predicting changes in temperate forest budburst using continental-scale observations and models. *Geophysical Research Letters*, 40, 359–364. <https://doi.org/10.1029/2012GL054431>
- Julien, Y., & Sobrino, J. (2009). Global land surface phenology trends from GIMMS database. *International Journal of Remote Sensing*, 30(13), 3495–3513. <https://doi.org/10.1080/01431160802562255>
- Keenan, T. F., Gray, J., Friedl, M. A., Toomey, M., Bohrer, G., Hollinger, D. Y., et al. (2014). Net carbon uptake has increased through warming-induced changes in temperate forest phenology. *Nature Climate Change*, 4(7), 598–604. <https://doi.org/10.1038/nclimate2253>
- Körner, C., & Basler, D. (2010). Phenology under global warming. *Science*, 327(5972), 1461–1462. <https://doi.org/10.1126/science.1186473>
- Kramer, K. (1994). Selecting a model to predict the onset of growth of *Fagus sylvatica*. *Journal of Applied Ecology*, 31(1), 172–181. <https://doi.org/10.2307/2404609>
- Laube, J., Sparks, T. H., Estrella, N., Hofler, J., Ankerst, D. P., & Menzel, A. (2014). Chilling outweighs photoperiod in preventing precocious spring development. *Global Change Biology*, 20(1), 170–182. <https://doi.org/10.1111/gcb.12360>
- Liu, Q., Fu, Y. H., Liu, Y., Janssens, I. A., & Piao, S. (2018). Simulating the onset of spring vegetation growth across the northern hemisphere. *Global Change Biology*, 24(3), 1342–1356. <https://doi.org/10.1111/gcb.13954>
- Liu, Q., Fu, Y. H., Zeng, Z., Huang, M., Li, X., & Piao, S. (2016). Temperature, precipitation, and insolation effects on autumn vegetation phenology in temperate China. *Global Change Biology*, 22(2), 644–655. <https://doi.org/10.1111/gcb.13081>
- Liu, Q., Fu, Y. H., Zhu, Z., Liu, Y., Liu, Z., Huang, M., Janssens, I. A., et al. (2016). Delayed autumn phenology in the northern hemisphere is related to change in both climate and spring phenology. *Global Change Biology*, 22(11), 3702–3711. <https://doi.org/10.1111/gcb.13311>
- MacBean, N., Maignan, F., Peylin, P., Bacour, C., Bréon, F. M., & Ciais, P. (2015). Using satellite data to improve the leaf phenology of a global terrestrial biosphere model. *Biogeosciences*, 12(23), 7185–7208. <https://doi.org/10.5194/bg-12-7185-2015>
- Martinez-Cantin, R. (2014). BayesOpt: A Bayesian optimization library for nonlinear optimization, experimental design and bandits. *Journal of Machine Learning Research*, 15(1), 3735–3739.
- Melaas, E. K., Friedl, M. A., & Richardson, A. D. (2015). Multi-scale modeling of spring phenology across deciduous forests in the eastern United States. *Global Change Biology*, 22(2), 792–805.
- Menzel, A., Sparks, T. H., Estrella, N., Koch, E., Aasa, A., Ahas, R., et al. (2006). European phenological response to climate change matches the warming pattern. *Global Change Biology*, 12(10), 1969–1976. <https://doi.org/10.1111/j.1365-2486.2006.01193.x>

- Mitchell, T. D., & Jones, P. D. (2005). An improved method of constructing a database of monthly climate observations and associated high-resolution grids. *International Journal of Climatology*, 25(6), 693–712. <https://doi.org/10.1002/joc.1181>
- Murray, M., Cannell, M., & Smith, R. (1989). Date of budburst of fifteen tree species in Britain following climatic warming. *Journal of Applied Ecology*, 26(2), 693–700. <https://doi.org/10.2307/2404093>
- New, M., Hulme, M., & Jones, P. (2000). Representing twentieth-century space-time climate variability. Part II: Development of 1901–96 monthly grids of terrestrial surface climate. *Journal of Climate*, 13(13), 2217–2238. [https://doi.org/10.1175/1520-0442\(2000\)013<2217:RTCSTC>2.0.CO;2](https://doi.org/10.1175/1520-0442(2000)013<2217:RTCSTC>2.0.CO;2)
- Ostle, N. J., Smith, P., Fisher, R., Woodward, F. I., Fisher, J. B., Smith, J. U., et al. (2009). Integrating plant–soil interactions into global carbon cycle models. *Journal of Ecology*, 97(5), 851–863. <https://doi.org/10.1111/j.1365-2745.2009.01547.x>
- Peñuelas, J., & Filella, I. (2001). Responses to a warming world. *Science*, 294(5543), 793–795. <https://doi.org/10.1126/science.1066860>
- Peñuelas, J., & Filella, I. (2009). Phenology feedbacks on climate change. *Science*, 324(5929), 887–888. <https://doi.org/10.1126/science.1173004>
- Piao, S., Fang, J., Zhou, L., Ciais, P., & Zhu, B. (2006). Variations in satellite-derived phenology in China's temperate vegetation. *Global Change Biology*, 12(4), 672–685. <https://doi.org/10.1111/j.1365-2486.2006.01123.x>
- Piao, S., Friedlingstein, P., Ciais, P., Viovy, N., & Demarty, J. (2007). Growing season extension and its impact on terrestrial carbon cycle in the northern hemisphere over the past 2 decades. *Global Biogeochemical Cycles*, 21, GB3018. <https://doi.org/10.1029/2006GB002888>
- Piao, S., Liu, Z., Wang, T., Peng, S., Ciais, P., Huang, M., et al. (2017). Weakening temperature control on the interannual variations of spring carbon uptake across northern lands. *Nature Climate Change*, 7(5), 359–363. <https://doi.org/10.1038/nclimate3277>
- Piao, S., Tan, J., Chen, A., Fu, Y. H., Ciais, P., Liu, Q., et al. (2015). Leaf onset in the northern hemisphere triggered by daytime temperature. *Nature Communications*, 6(1), 6911. <https://doi.org/10.1038/ncomms7911>
- Pinzon, J. E., & Tucker, C. J. (2014). A non-stationary 1981–2012 AVHRR NDVI_{3g} time series. *Remote Sensing*, 6(8), 6929–6960. <https://doi.org/10.3390/rs6086929>
- Raftery, A. E., Gneiting, T., Balabdaoui, F., & Polakowski, M. (2005). Using Bayesian model averaging to calibrate forecast ensembles. *Monthly Weather Review*, 133(5), 1155–1174. <https://doi.org/10.1175/MWR2906.1>
- Raftery, A. E., & Zheng, Y. (2003). Discussion: Performance of Bayesian model averaging. *Journal of the American Statistical Association*, 98(464), 931–938. <https://doi.org/10.1198/016214503000000891>
- Richardson, A. D., Anderson, R. S., Arain, M. A., Barr, A. G., Bohrer, G., Chen, G., et al. (2012). Terrestrial biosphere models need better representation of vegetation phenology: Results from the North American carbon program site synthesis. *Global Change Biology*, 18(2), 566–584. <https://doi.org/10.1111/j.1365-2486.2011.02562.x>
- Richardson, A. D., Black, T. A., Ciais, P., Delbart, N., Friedl, M. A., Gobron, N., et al. (2010). Influence of spring and autumn phenological transitions on forest ecosystem productivity. *Philosophical Transactions of the Royal Society, B: Biological Sciences*, 365(1555), 3227–3246. <https://doi.org/10.1098/rstb.2010.0102>
- Richardson, A. D., Keenan, T. F., Migliavacca, M., Ryu, Y., Sonnentag, O., & Toomey, M. (2013). Climate change, phenology, and phenological control of vegetation feedbacks to the climate system. *Agricultural and Forest Meteorology*, 169(2013), 156–173. <https://doi.org/10.1016/j.agrformet.2012.09.012>
- Schulzweida, U. (2013). Climate data operators: A large tool set for working on climate and NWP model data. Retrieved from <http://code.zmaw.de/projects/cdo>
- Schwartz, M. D., Ahas, R., & Aasa, A. (2006). Onset of spring starting earlier across the northern hemisphere. *Global Change Biology*, 12(2), 343–351. <https://doi.org/10.1111/j.1365-2486.2005.01097.x>
- Schwartz, M. D., & Hanes, J. M. (2010). Continental-scale phenology: Warming and chilling. *International Journal of Climatology*, 30(11), 1595–1598. <https://doi.org/10.1002/joc.2014>
- Sitch, S., Smith, B., Prentice, I. C., Arneth, A., Bondeau, A., Cramer, W., et al. (2003). Evaluation of ecosystem dynamics, plant geography and terrestrial carbon cycling in the LPJ dynamic global vegetation model. *Global Change Biology*, 9(2), 161–185. <https://doi.org/10.1046/j.1365-2486.2003.00569.x>
- Stéfanon, M., Drobinski, P., D'Andrea, F., & Noblet-Ducoudré, N. (2012). Effects of interactive vegetation phenology on the 2003 summer heat waves. *Journal of Geophysical Research*, 117, D24103. <https://doi.org/10.1029/2012JD018187>
- Thornton, P. E., Law, B. E., Gholz, H. L., Clark, K. L., Falge, E., Ellsworth, D. S., et al. (2002). Modeling and measuring the effects of disturbance history and climate on carbon and water budgets in evergreen needleleaf forests. *Agricultural and Forest Meteorology*, 113(1–4), 185–222. [https://doi.org/10.1016/S0168-1923\(02\)00108-9](https://doi.org/10.1016/S0168-1923(02)00108-9)
- Vandvik, V., Halbritter, A. H., & Telford, R. J. (2018). Greening up the mountain. *Proceedings of the National Academy of Sciences of the United States of America*, 115(5), 833–835. <https://doi.org/10.1073/pnas.1721285115>
- Vitasse, Y., Signarbieux, C., & Fu, Y. H. (2018). Global warming leads to more uniform spring phenology across elevations. *Proceedings of the National Academy of Sciences of the United States of America*, 115(5), 1004–1008. <https://doi.org/10.1073/pnas.1717342115>
- Vrugt, J. A., & Robinson, B. A. (2007). Treatment of uncertainty using ensemble methods: Comparison of sequential data assimilation and Bayesian model averaging. *Water Resources Research*, 43, W01411. <https://doi.org/10.1029/2005WR004838>
- Wang, C., Tang, Y., & Chen, J. (2016). Plant phenological synchrony increases under rapid within-spring warming. *Scientific Reports*, 6(1), 25460. <https://doi.org/10.1038/srep25460>
- Wang, T., Ottlé, C., Peng, S., Janssens, I. A., Lin, X., Poulter, B., et al. (2014). The influence of local spring temperature variance on temperature sensitivity of spring phenology. *Global Change Biology*, 20(5), 1473–1480. <https://doi.org/10.1111/gcb.12509>
- Way, D. A., & Montgomery, R. A. (2015). Photoperiod constraints on tree phenology, performance and migration in a warming world. *Plant, Cell & Environment*, 38(9), 1725–1736. <https://doi.org/10.1111/pce.12431>
- Wolkovich, E. M., Cook, B., Allen, J., Crimmins, T., Betancourt, J., Travers, S., et al. (2012). Warming experiments underpredict plant phenological responses to climate change. *Nature*, 485(7399), 494–497. <https://doi.org/10.1038/nature11014>
- Zhang, X., Friedl, M. A., Schaaf, C. B., Strahler, A. H., Hodges, J. C., Gao, F., et al. (2003). Monitoring vegetation phenology using MODIS. *Remote Sensing of Environment*, 84(3), 471–475. [https://doi.org/10.1016/S0034-4257\(02\)00135-9](https://doi.org/10.1016/S0034-4257(02)00135-9)
- Zohner, C. M., Benito, B. M., Svenning, J.-C., & Renner, S. S. (2016). Day length unlikely to constrain climate-driven shifts in leaf-out times of northern woody plants. *Nature Climate Change*, 6(12), 1120–1123. <https://doi.org/10.1038/nclimate3138>